ARTICLES

Study on Two-Component Matrix Formed by Coadsorption of Aromatic and Long Chain Mercaptans on Gold

Hao-Li Zhang, Miao Chen, and Hu-Lin Li*

Department of Chemistry, Lanzhou University, Lanzhou 730000, China

Received: April 28, 1999; In Final Form: August 30, 1999

Binary monolayers comprised of mercaptopyrimidine (MP) and 1-dodecanethiol ($C_{12}SH$) in varying ratios were prepared on gold surfaces by self-assembly and then characterized using reflection absorption FTIR spectroscopic (RA-IR), electrochemical, and wettability measurements. The RA-IR results revealed that the coverage of MP in the mixed monolayer is controlled by its composition in solution. The adsorption of mixed monolayers appears to be kinetically controlled. The wettability of mixed monolayers indicated that the surface fraction of $C_{12}SH$ exposed to the probe liquid exceeded that of its mole fraction in the monolayer. Electrochemical measurements demonstrated that the permeabilities of various quinone probes into the mixed self-assembled monolayers (SAMs) were dominated by their geometry. The origination of the geometry-dependent permeability of probes is believed to be related to the average size of MP domain in SAMs.

1. Introduction

Interest in the preparation of highly organized surface-bonded molecular assemblies with molecular level control over the structure order and composition has grown considerably in recent years.[1−5] The development of self-assembled monolayers (SAMs) has received particular attention. SAMs prepared from long chain alkanethiols are well-known examples of two-dimensional ordered structures, in which the chains appear to approach the ideal rigid-rod limit of all-trans conformations with a uniform tilt angle.[1−5] In practice, however, defects are always present. In some cases, a large number of partially disordered structural phases will arise, ranging from homogeneous films of uniform density to heterogeneous films of macroscopic patches of organized adsorbate.[6,7] The heterogeneity of the monolayers can strongly influence their surface properties, such as wetting by liquid,[8] and charge transport in electrochemical systems.[9]

Recently, controlling surface properties by heterogeneity in monolayers has attracted increasing attention.[10−12] A variety of preparations are possible,[13−17] but the most widely used is self-assembly of multicomponent ω-functionalized alkanethiols ($HS(CH_2)_nX$) from solution onto gold surfaces,[4,18,19] with various terminated groups such as CH_3, CO_2H, OH, CN, CO_2CH_3, and ferrocene.[20−23] Such films allow many possibilities for systematic studies of a wide range of interfacial phenomena including wetting,[24,25] electron transfer,[22,23] protein adsorption,[26,27] molecular recognition,[28] and multilayer film formation.[29,30] Another useful structural variation involves assembly of mixed chain length alkanethiols providing control of both vertical and horizontal distributions of functionality with respect to the surface plane. Wetting studies on mixed chain length SAMs[11,12,14,31,32] indicated that protrusion of long chain segments into the wetting medium decreases the wetting effects of the shorter chain segments.

Two-component SAMs have been widely investigated.[15,21,33−35] However, the fundamental structure−property correlation of binary SAMs as well as the preparation conditions for the synthesis of specific architectures is still under investigation. Factors governing the formation of mixed self-assembled monolayers currently are not well understood. It is generally accepted that long chain alkanethiols are preferentially adsorbed compared to short chain alkanethiols and that monolayer composition appears to be thermodynamically controlled.[33,36] For example, Chidsey et al.[22] showed that two-component SAMs can be enriched slightly in one component by equilibrating the monolayer in a solution containing the desired component. On the basis of this result, the authors concluded that molecules adsorbed at defect sites are labile and can exchange with solution-phase species, while molecules adsorbed at terraces were stable and did not exchange to any significant extent. This finding has been confirmed by Creager[37] and Whitesides.[21]

Herein, we investigated two-component SAMs prepared by coadsorption of long chain alkanethiol and aromatic mercaptan from solution. Our objectives were (1) to study the factors determining the assembly of a long chain alkanethiol and an aromatic mercaptan into a mixed monolayer and (2) to find a method to control the surface composition and distribution of these two components. We have also studied the molecular recognition properties of this matrix. Binary matrices that incorporate molecular "gate" sites are being developed as a way of designing monolayers with molecular recognition properties.[38−40] In these matrices, long chain components could act as a framework, preventing a probe molecule from penetrating through the monolayer membrane,[41] and the small components

* To whom correspondence should be addressed. E-mail: Lihl@lzu.edu.cn. Tel: +86-931-8912517. Fax: +86-931-8911100.

10.1021/jp991391a CCC: $19.00 © 2000 American Chemical Society
Published on Web 12/16/1999

could act as a template that induces active sites within the inert framework that permit probe molecule penetration.[42]

2. Experimental Section

Reflection Absorption Infrared Spectroscopy (RA-IR). All infrared spectra were recorded on a Perkin-Elmer System 2000 FT-IR spectrophotometer equipped with a liquid-N_2-cooled MCT detector. A SPECAC variable angle reflection attachment was used for reflection adsorption measurements. The p-polarized infrared beam by a PERKIN ELMER wire-grid polarizer was incident on the sample plane at 85° (near grazing angle) from the surface normal. The resolution of the system was set to be 4 cm^{-1}, and usually 500 interferograms were collected to achieve an acceptable signal-to-noise ratio. The sample chamber was purged with nitrogen to eliminate the interference of the absorption of water vapor in air.

Wettability Measurements. Contact-angle measurements were performed with a JJC-II contact-angle goniometer under ambient conditions (21−23 °C, 50−60% relative humidity) using yellow light to illuminate the liquid droplet. The contact angles were obtained by expanding a droplet from a micro-syringe until it advanced smoothly across the surface and then measuring the angle 10−20 s after expansion. At least four results were read for each sample.

Sample Preparation. The substrates employed in RA-IR spectroscopic studies and wettability measurements were prepared by evaporating 200 nm of gold (99.99%) onto a glass slide (7.5 × 2.5 cm) precoated with 10−15 nm of chromium at the evaporation rate of 0.1 nm/s. The base pressure was always less than 3.5×10^{-6} Torr and the evaporation pressure less than 5.5×10^{-6} Torr. The gold slides were precleaned in a heated solution of 1:4 30% H_2O_2 in concentrated H_2SO_4. *Caution: A solution of H_2O_2 in H_2SO_4 is very strong oxidant and reacts violently with many organic materials. It should be handled with extreme care*. The self-assembled monolayers (SAMs) were prepared by immersing cleaned gold slides into a series of 1.0 mmol/L ethanol solution of 1-dodecanethiol ($C_{12}SH$) and 2-mercaptopyrimidine (MP) with different component ratios over 12 h to reach a saturated coverage. Afterward, the monolayers were washed with ethanol and dried in N_2 prior to the characterization.

Electrochemical Measurements. The electrochemical experiments were carried out with a BAS-100B electrochemical analyzer. A conventional three-electrodes system was used throughout. All potentials were reported versus a Ag/AgCl (3 mol/L KCl) reference electrode. A platinum wire was employed as the counter electrode. The working electrode was a bare or a SAM-modified gold disk electrode (geometric area: 0.0314 cm^2). The gold electrode was cleaned by potential scanning in 0.5 mol·L^{-1} H_2SO_4 between −200mV and 1400 mV until a stable cyclic voltammogram was obtained. After the cleaning processing, the substrates were rinsed with doubly distilled water and ethanol and then immediately immersed into assembling solution.

The double-layer capacitance of the SAM-modified electrodes were measured by cyclic voltammetry[43,44] using the equation

$$C_{dl} = i_c \cdot v^{-1} \cdot A^{-1} \quad (1)$$

where C_{dl} is the double-layer capacitance, i_c is the charging current, v is the scan rate, and A is the electrode surface area. The true area of the gold electrode determined by cyclic voltammogram[45] in 0.5 mol·L^{-1} H_2SO_4 is 0.039 cm^2.

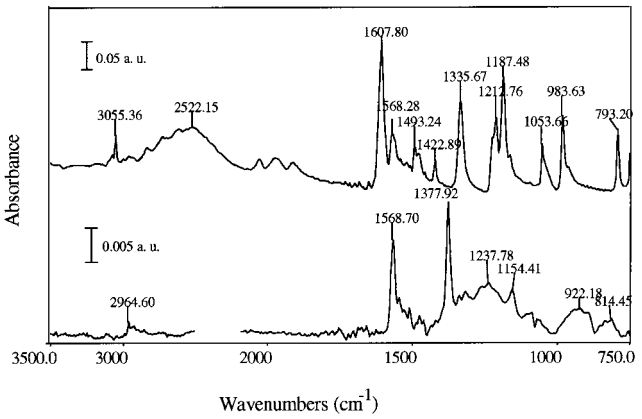

Figure 1. Comparison of the transmission IR spectrum (top) of MP in KBr pellet and the RA-IR spectrum (bottom) of pure MP SAM.

SCHEME 1: 2-Mercaptopyrimidine and the Hydrogen-Bonded Dimer of Its Thione Form

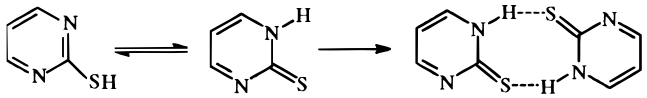

3. Results

3.1. Infrared Spectra. Infrared spectroscopy has become a routine method to obtain the structural information of monolayers because it gives much information about molecular orientation and packing density of the films. Research on mixed monolayers from the alkanethiols with variations in the length, headgroup, tail group, and solvent has been reported.[18]

3.1.1. RA-IR of MP on Gold. The RA-IR spectrum of the MP SAM is shown in Figure 1. For comparison, a transmission spectrum of the same sample dispersed in KBr pellet is also shown.

The vibrational spectra of substituted pyrimidine have been extensively studied by many groups.[46−51] Herein, we only give a general introduction. It is well-known that organic molecules bearing a mobile H atom undergo rapid and facile tautomeric transformations.[52] It is also generally accepted that, at ambient condition, the pyrimidine substituted at the 2 or 4 position by potentially tautomeric groups (OH or SH) exists in lactam or thione forms rather than in lactim or thiol forms in solution.[46−52] However, the preferred form in the solid state is still under investigation. It is clearly understood from X-ray crystallography that 2-mercaptopyridine exists as a H-bonded dimer of its thione form tautomer in the solid state.[53] Similarly, it is proposed that MP actually exists as a H-bonded dimer of 2(1*H*)-pyrimidinethione in the solid state (Scheme 1).

The sharp, medium intensity peak at 3055 cm^{-1} is characteristic for stretching of C−H on the heterocyclic ring of the pyrimidine. The broad absorption band around 2520 cm^{-1} is therefore assigned to the stretching of the N−H bond in 2(1*H*)-pyrimidinethione, which is strongly hydrogen bonded. The three bands near 2000 cm^{-1} may be assigned as a result of Fermi resonance and overtones of the ν(N−H) mode. As suggested by Kwiatkowski,[49] the strong band at 1608 cm^{-1} is assigned to the N−H in-plane bending vibration. The stretching of C═S and N−H out-of-plane deformation are observed at 1213 and 1053 cm^{-1}, respectively. The other medium or intense bands falling in the region from 900 to 1600 cm^{-1} are attributed to the ring stretching and deformation. The C−H out-of-plane deformation is observed at 793 cm^{-1} as a moderately intense absorption.

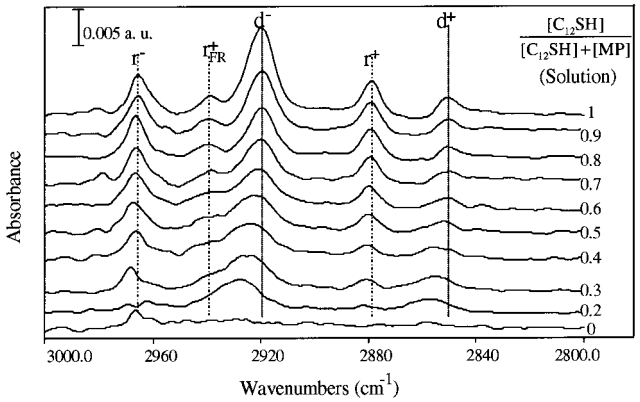

Figure 2. RA-IR spectra (C−H stretching region) of SAMs on gold derived from ethanolic solutions containing mixtures of $C_{12}SH$ and MP. The compositions of the assembling solutions are illustrated as mole fraction of $C_{12}SH$ in solution.

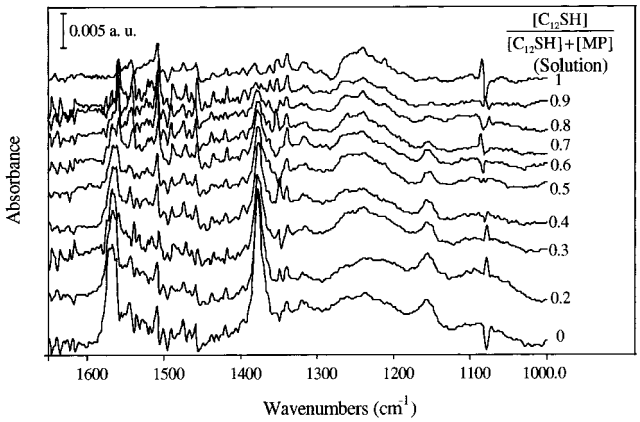

Figure 3. RA-IR spectra (middle frequency region) of SAMs on gold derived from ethanolic solutions containing mixtures of $C_{12}SH$ and MP. The compositions of the assembling solutions are illustrated as mole fraction of $C_{12}SH$ in solution.

The RA-IR spectrum of MP SAM is remarkably different from the spectrum of it in KBr, suggesting that the MP molecule undergoes great changes after being adsorbed onto the gold surface. The first feature of the RA spectrum is the absence of absorption of stretching and in-plane bending vibration modes of the N−H group, which appeared around 2520 and 1607 cm^{-1}, respectively, in the transmission spectrum. We believe that the absence of the two bands strongly indicates that the MP molecule in the SAM is no longer in thione form. Another feature is that the prominent band at 1335 cm^{-1} in the transmission spectrum moved to 1377 cm^{-1} in the RA-IR spectrum. Note that the skeleton vibration of 2-thiomethylpyrimidine gives rise to a strong band around 1380 cm^{-1};[47] we propose that the MP molecule at the gold surface exists as a form analogous to the 2-thioalkyl-substituted pyrimidine. In summary, the difference between the spectrum of the isotropic sample of MP in KBr and the spectrum of its SAM reveals the changes of the MP from the thione form in the polycrystalline state to the sulfide (R−S−Au) form in the SAM.

3.1.2. RA-IR Spectra of Mixed SAMs. Representative RA-IR spectra of mixed SAMs prepared from the solutions with different ratios of $C_{12}SH$ and MP are shown in Figure 2 over the 3000−2800 cm^{-1} region. As the mole fraction of $C_{12}SH$ in the monolayer decreases (i.e., as the mole fraction of MP increases), several trends can be observed in the IR data. A considerable part of the infrared work on SAMs has been devoted to the C−H stretching vibrations in methyl and methylene groups, since they can provide important information about the chain conformation and orientation. It is well-known that the position, the intensity, and the peak shape of d^+ (methylene symmetric stretching) and d^- (methylene asymmetric stretching) bands are sensitive to the phase state of the polyethylene chain.[54,55] A disordered "liquidlike" SAM is expected to give broader absorption bands and exhibit higher frequency than that in the crystalline state.[56]

The first feature of the spectra is that there is a significant decrease of intensities of the C−H stretching vibration modes in both methyl and methylene groups while the ratio of $C_{12}SH$ decreases. The variation of the intensities is directly related to the mole fraction of the $C_{12}SH$ in the series of SAMs, so that the changes observed clearly indicate that SAMs prepared from the solutions that have more $C_{12}SH$ have higher weight of $C_{12}SH$. However, the absorbance in RA-IR spectra is also affected by the molecular orientation at the surface and the microenvironment the molecules are in. For example, a higher tilting angle of the polyethylene chain will lead to more projection of the d^+ and d^- modes in the direction of the surface normal and therefore give higher absorbance. In our case, we cannot assume that structure of the polymethylene chain is conserved with the presence of the MP molecule in the film. Therefore, the intensity of the C−H stretching modes in this region cannot be used for quantitative determination of the surface composition. Another interesting feature of Figure 2 is that the position and width of peaks in this region change with surface composition. The spectrum of pure monolayer of $C_{12}SH$ is identical to what has been previously observed for fairly well-ordered and densely packed monolayer on the surface by the positions of d^+ and d^- modes at 2919 and 2850 cm^{-1}, respectively.[54,55] The above two bands shift to higher frequencies and become broader when the ratio of MP in the assembling solution increases. This shift is consistent with a transition toward a less ordered monolayer structure.[43] Hence, it can be concluded that more small molecules (MP in our case) in the SAMs lead to more significant perturbation to the longer alkanethiols ($C_{12}SH$ here). It is also notable that the position of methyl group asymmetric stretching (r^+) and symmetric stretching (r^-) modes also shifts toward higher frequency as the weight of MP in the monolayers increases. Up to now, the interpretation of the shift of r^+ and r^- bands is not very clear. Stole and Porter had reported that the position of methyl stretching modes in methyl-terminated alkanethiol SAMs shifted toward a lower frequencies direction when contacted with condensed phases (water, methanol, and CCl_4) compared with that of it contacted with air.[57] And they attributed the shifts to the solvent-induced disorder of the film. However, arguments recently came from Laibinis and Whidesides' investigations on mixed SAMs of alkanethiols with different lengths, in which they suggested that the shifts of both r^+ and r^- bands to lower wavenumber should indicate an increasing order of alkyl chain.[16,36] It seems that our observation supports the later interpretation.

The correlation between the surface composition and the composition of the corresponding assembling solution can be evaluated from the middle region (1650−1000 cm^{-1}) of the RA-IR spectra (Figure 3). The bands assigned to the in-plane vibrations of the pyrimidine ring are clearly observed at 1566 and 1378 cm^{-1}, respectively. The intensities of the two peaks increase with the increase of the content of MP. No obvious changes in either position or width of these peaks are observed in these spectra. It was suggested by Laibinis[16,36] that the dilution by the longer chained component does not constitute a major perturbation of the local molecular environment of the shorter molecules in the SAMs. Therefore, it is reasonable to assume

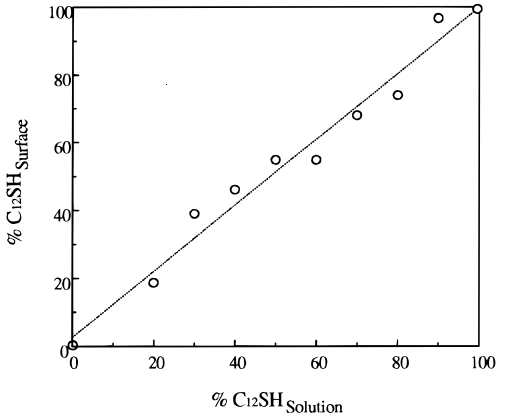

Figure 4. Relationship between the surface composition and the solution composition. The surface composition is evaluated from the integrated intensity of the skeleton vibration mode of MP at 1378 cm^{-1} (see Figure 3). The dotted line demonstrates a result of linear regression.

that the intensities of the two peaks associated with MP are only related to the weight of MP in SAMs. The estimated surface composition evaluated from the integrated intensity of the 1378 cm^{-1} band is displayed in Figure 4 as a function of the mole fraction of $C_{12}SH$ in the assembling solution. A roughly linear relationship between the surface composition and the solution composition is found in Figure 4, which indicates that the surface compositions of the mixed SAMs prepared under our conditions are approximately the same as the composition of the assembling solution. This result suggested that the adsorption of the two components from solution to surface is more likely to be controlled kinetically rather than thermodynamically.

Another question is what the distribution of $C_{12}SH$ and MP molecules in the mixed SAMs is, well-mixed or phase-separated. We cannot obtain a clear interpretation from these spectra. We are inclined to believe that phase separation occurs in our system. As we have observed in Figure 2, the position and width of d^+ and d^- modes of the CH_2 groups exhibit shift with the changes in the surface composition. The widening and the shifts of d^+ and d^- bands are explained as the increase of the weight of adsorption at the higher frequency edge which relates to the disordered chain. On this basis, the existence of the intensity at 2919 cm^{-1} in the spectra of mixed SAMs from the solution composed of $C_{12}SH$ more than 20% is mostly like to indicate the presence of ordered alkanethiolate domain structure in these SAMs. The formation of the domain structure should be attributed to thermodynamic reasons, that the well-mixed solid solution of alkanethiol and heterocyclic mercaptan is not thermodynamically favored because it will decrease the van der Waals attraction among the alkyl chains.

3.2. Wettability. The quality and microscopic structure of the mixed SAMs were also estimated from wetting measurements. Young described the relationship between the free energy of the surface and a unique contact angle, under ideal conditions, for a system in equilibrium[58,59] as

$$\gamma_{LV} \cos \theta = \gamma_{SV} - \gamma_{SL} \quad (2)$$

where θ is the contact angle at the three-phase interface while the γ_{LV}, γ_{SV}, and γ_{SL} are surface-free energies at the liquid−vapor interface, solid−vapor interface, and solid−liquid interface, respectively. Monolayers containing exposed polar groups and disordered monolayers have much lower contact angles. If the mixed monolayers containing two components are homogeneous and the two components affect surface wettability independently, the Cassie equation is appropriate for interpretation of wettability results[60,61]

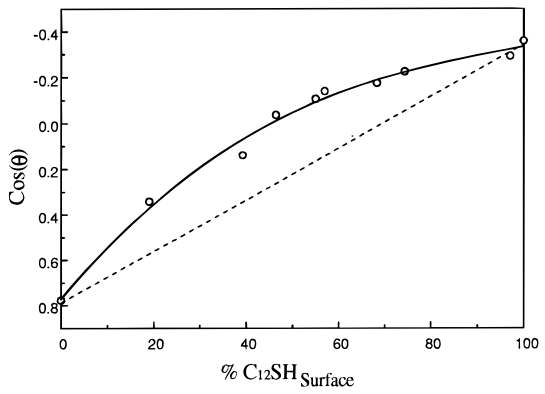

Figure 5. Cosines of contact angle (θ) of pure water on SAMs-modified surface plotted as a function of the percentage of $C_{12}SH$ in SAMs. The solid line is shown as a guide to the eye, and the dashed line represents an expected linear relationship.

$$\cos \theta = f_1 \cos \theta_1 + f_2 \cos \theta_2 \quad (3)$$

where θ is the contact angle of a liquid on the heterogeneous surface, f_1 and f_2 are the fractions of the two types of chemical groups at the surface, and θ_1 and θ_2 are the contact angles of this liquid on the pure homogeneous surfaces of the two functional groups, respectively. Consequently, changes in cos θ are expected to be linearly dependent on the composition of the surface for an ideal surface.[62−69] Hence, the composition and quality of a monolayer are usually checked quickly and easily with this technique.[66−68]

The cosines of contact angles of pure water on freshly prepared monolayers composed of mixtures of MP and $C_{12}SH$ are shown as a function of the surface composition (Figure 5). The SAMs become more hydrophobic as the $C_{12}SH$ content increases. The obviously nonlinear behavior displayed in Figure 5 indicates that the wettability of SAMs mixed with $C_{12}SH$ and MP is highly nonideal.

The relation between surface wettability and the surface composition of the mixed SAMs demonstrates the complexity of the interactions at film, air, and probe liquid three-phases interface. Bain and his colleagues studied the wettability of SAMs mixed with alkanethiols of similar chain length terminated by the methyl group and other polar groups. They found that the curve of cos θ against surface composition usually appeared concavely rather than convexly.[16,18,36] The mixed SAMs considered here are also consistent with a polar component (MP) and a low surface energy component ($C_{12}SH$). However, in contrast with that observed by Bain, Figure 5 demonstrates a convex curve which indicates that the SAMs mixed with MP and $C_{12}SH$ are more hydrophobic than that predicted by Cassie's equation. The major difference between our system and Bain's is that the length of the two components researched here is much different; the $C_{12}SH$ molecule is about two times longer than the MP molecule. As our RA-IR spectral results suggest, incorporation of MP into the monolayer significantly perturbs the local environment of $C_{12}SH$ and causes disorder in the monolayers. The $C_{12}SH$ molecules do not hold their orientation as in homogeneous film and extend above the MP molecules in the mixed SAMs (Scheme 2). Consequently, only part of the adsorbed MP molecule can be contacted by the probe liquid owing to the covering effect of $C_{12}SH$. The C_{12}-SH molecule extending above the MP molecule will not be in its usual gauche conformation. This will result in exposure of the probe liquid to methylene groups along the alkyl chain.

SCHEME 2: Schematic Illustration of the Structure of Two-Component Matrix Formed by Long Chain and Aromatic Mercaptans

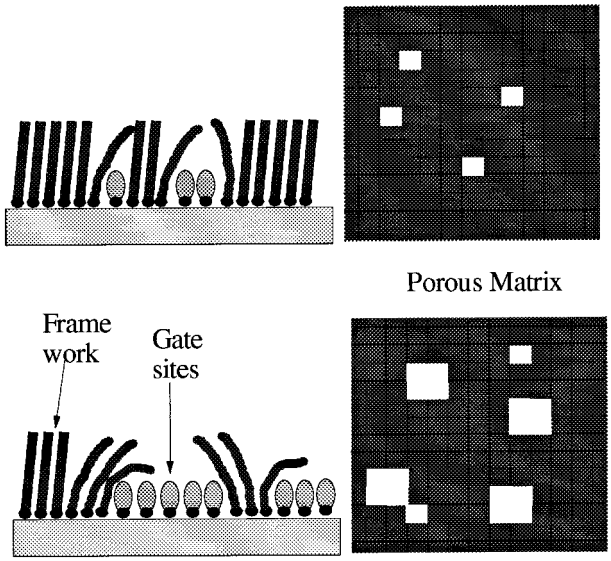

Although exposed methylene groups are more available for wetting, they are more hydrophobic than the terminal methyl group. Therefore, SAMs comprised of mixtures of MP and $C_{12}SH$ are more hydrophobic than expected by Cassie's equation.

3.3. Electrochemical Investigation. The RA-IR spectroscopic and wettability measurement results demonstrate that binary functional composite monolayers have been prepared. The ratio of the two constituents in the monolayers could be easily controlled and manipulated. The film structure changed dramatically with composition. We next examined the electrochemical properties of the mixed SAMs using a series of probe molecules to gain access to the gold surface at the molecular level.

3.3.1. Capacitance. Measurement of capacitance has been used as a method to verify the quality of molecular packing in SAMs. The coating of a gold electrode with an alkanethiolate monolayer causes a dramatic decrease in the electrolyte/electrode capacitance. The capacitance drops from values larger than 50 $\mu F \cdot cm^{-2}$ to about 0.7 $\mu F \cdot cm^{-2}$ for an octadecanethiolate-covered electrode.[43,70,71] The latter capacitance is independent of the scan rate or frequency, the type of electrolyte, and the applied potential in a large potential range (−1.0 to +0.8 V, vs SCE). The capacitance data is usually simplified[43] to the parallel plate capacitor model, in which the monolayer-coated electrode is modeled to be a capacitor with the gold electrode surface and the electrolyte solution forming the two conducting plates of the capacitor. In this case the capacitance can be described by the following equations, where ϵ_r is the relative dielectric constant of the monolayer; ϵ_0, the dielectric constant of vacuum, and d_{eff}, the effective thickness of the monolayer.

$$C = \epsilon_0 \epsilon_r / d_{eff} \quad (4)$$

Effective thicknesses are calculated for long chain alkanethiolates that are only slightly smaller than the ellipsometrically determined thickness, assuming the relative dielectric constant of the monolayer equals that of polyethylene ($\epsilon_r = 2.3$). This implies that the bulk of these assemblies is impermeable to electrolyte intrusion.[43,72]

The double-layer capacitance of clean gold electrode was determined as 65.5 $\mu F \cdot cm^{-2}$ in 0.1 $mol \cdot L^{-1}$ H_2SO_4 solution at the potential of 50 mV, which is in agreement with the result of Miller.[72,73] The capacitances of the mixed monolayers were determined (Figure 6) within 10% relative error. It can be seen that with increasing content of MP in the monolayer the capacitance increases dramatically. The changes in capacitance indicate a transition of film structure. While the content of MP increases, the average ϵ_r of the film should increase and the d_{eff} decrease. Therefore, the film capacitance increases with the increase of MP content.

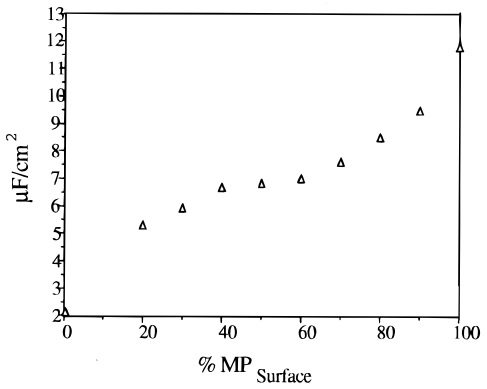

Figure 6. Plot of capacitance of the mixed monolayers against the corresponding percentage of MP content in SAMs.

3.3.2. Stability. The electrochemical stabilities of the mixed monolayer modified layer are determined in different supporting electrolytes. The potential window in which the SAMs-modified electrode is stable depends on the solution pH. For example, at pH 2.0 the anodic background current begins to increase at approximately 0.75 V and the cathodic at −0.3 V. The anodic limit is similar at higher pH. The cathodic limit is approximately 0.15 V more negative in neutral solutions. In the potential window of +0.65 to −0.3 V the background currents do not exceed 3 $\mu A/cm^2$. Electrode response and the background current do not change as long as the electrode is used in this potential window. The SAMs are damaged when the potential exceeds the limits, allowing large oxidation or reduction currents at positive and negative potentials, respectively. The damage is accompanied by the appearance of the characteristic reduction peak of gold oxide.[74]

3.3.3. Electrochemical Response of $Fe(CN)_6^{4-}$ on SAMs. Heterogeneous electron transfer of redox center on such membrane-modified electrodes is widely used as a conventional technology to test the integrality and packing density of the film. Portor and co-workers[54] reported that the thiols having alkyl chains longer than $n = 11$ formed densely packed monolayer assemblies with fully extended alkyl chains and hindered the electron transfer between metal surfaces and alkyl chain/electrolyte interface. The cyclic voltammogram (CV) of $Fe(CN)_6^{4-}$ on mixed SAMs in aqueous solution is shown in Figure 7. The anodic peak current decreased while the content of $C_{12}SH$ in the film increased, indicating an increase of the barrier effect of the films on the redox reaction of $Fe(CN)_6^{4-}$. The peak diminishes rapidly as the content $C_{12}SH$ in the film increases. In agreement with a previous report,[40] only a very small amount of $C_{12}SH$ (e.g., mole fraction about 30%) in the film is sufficient enough to inhibit the redox reaction of $Fe(CN)_6^{4-}$ at the electrode. This strongly suggests that the $C_{12}SH$ molecule occupies a larger area fraction in the film compared to its mole fraction.

3.3.4. Permselectivity of Quinones on SAMs. To probe the effect of the geometry contribution on the electrochemical response, the response of a series of structural analogues was

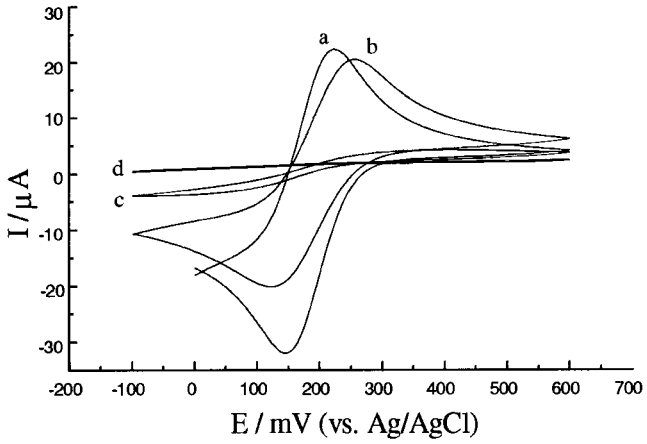

Figure 7. Cyclic voltammetric response of 1.0×10^{-3} mol/L $Fe(CN)_6^{4-}$ on bare gold (a) and gold modified with mixed SAMs containing 90% MP (b) and 70% MP (c), and gold modified with pure $C_{12}SH$ (d). The supporting electrolyte was 0.1 mol/L $NaClO_4$ solution, and scan rate was 100 mV/s.

investigated. The quinones 2,3,5,6-tetrachloride-1,4-benzoquinone (Cl_4-BQ), 2-methyl-1,4-naphthoquinone sulfonic acid sodium salt (VK_3), and 1,2-dihidroxyanthraquinine-3-sulfonic acid sodium salt (AQ-S) were adopted as electroactive probe molecules. The sulfonic acid sodium salts were chosen for their sufficiently high solubility in purely aqueous electrolyte. The electrochemical reactions of all the three probe molecules on bare gold electrode have been studied extensively.[75] All the CVs of quinones on gold were measured in neutral electrolyte so that the influences of charging could be ruled out.

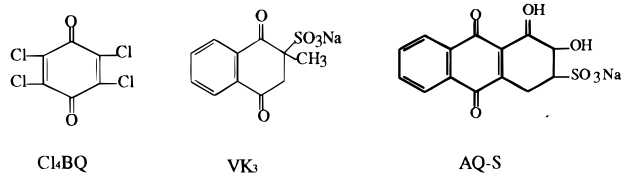

The CVs of Cl_4BQ on bare gold, on pure MP SAM, and on SAM containing 60% MP are shown in Figure 8. No significant difference is found between the CVs of Cl_4BQ on bare gold and pure MP SAM, suggesting that the MP-modified surface does not inhibit the electron transfer between gold electrode and Cl_4BQ. While the weight of MP decreased to 60%, the oxidation peak current of Cl_4BQ decreased to about 82% of that on pure MP SAM. Clearly, the electron-transfer reaction of Cl_4BQ on SAM-modified gold electrode could be modulated by the weight of MP in the mixed SAMs. From the CVs of VK_3 and AQ-S on gold and mixed SAMs (Figures 9 and 10), similar results could be obtained: the less the weight of MP in SAMs, the lower the redox current. However, the effects of surface composition on the responses of the three quinones are different. To access the reaction of a larger probe on mixed SAMs, more MP in SAMs is need. For example, when the mole fraction of MP in mixed monolayer was 80%, the reduction peak i_{pa} of VK_3 was only about 37% of the i_{pa} on pure MP SAM. In contrast, no redox response of AQ-S could be observed when the MP percentage was around 80%. Meanwhile, with decreasing MP percentage, all of the probe molecules' potential difference ($\Delta E_p = E_{pa} - E_{pc}$) increased, which indicates that the mass transfer was hindered.[76] Although the reaction mechanism of the three quinones on gold may differ, inducing slightly different shapes in the CV curves, we believe that the different electrochemical response of probe molecules on the mixed

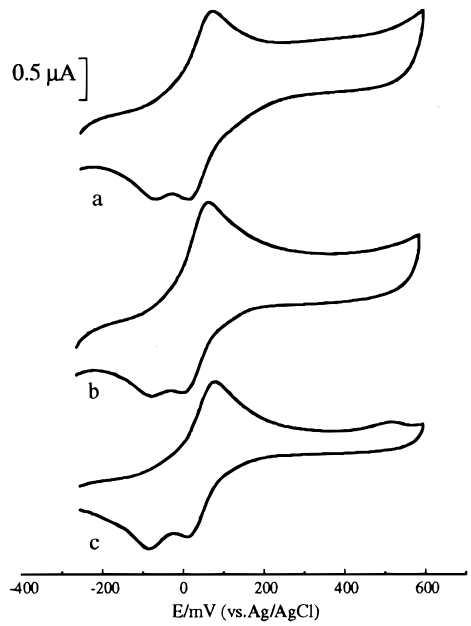

Figure 8. Cyclic voltammetric response of 5.0×10^{-4} mol/L Cl_4BQ on bare gold (a), gold modified with pure MP SAM (b), and gold modified with mixed SAMs containing 60% MP (c). The supporting electrolyte was 0.1 mol/L $NaClO_4$ with 0.025 mol/L phosphate buffer (pH 7.0). Scan rate: 50 mV/s.

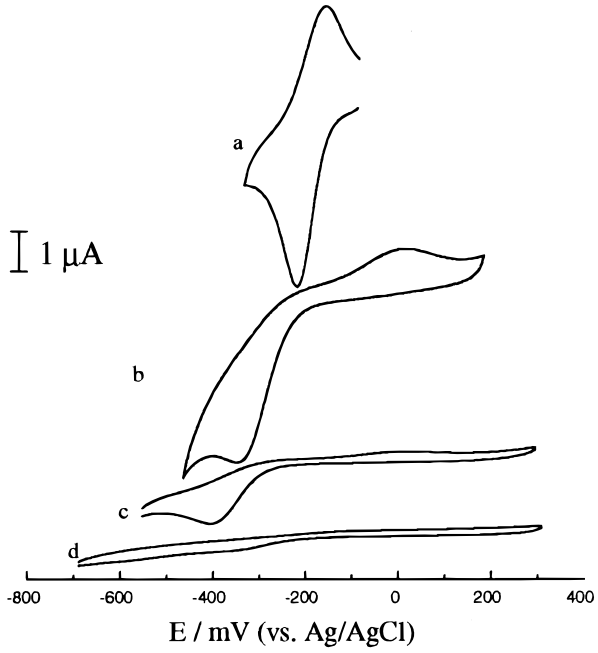

Figure 9. Cyclic voltammetric response of 5.0×10^{-4} mol/L VK_3 on bare gold (a), gold modified with pure MP SAM (b), and gold modified with mixed SAMs containing 80% MP (c) or 50% MP (d). The supporting electrolyte was 0.1 mol/L $NaClO_4$ and 0.025 mol/L phosphate buffer (pH 7.0). Scan rate was 50 mV/s.

SAMs is mainly attributed to their different ability to permeate the membrane.

For convenience, we used the ratio of I_p/I_p^0 for evaluating the permeability of the quinones on the mixed SAMs,[77] where I^0 represents the peak current of probes on pure MP SAM and I is the peak current of the same quinone on mixed SAMs. The peaks used in the measurement are cathode peak at +80 mV in the CV of Cl_4BQ and anodic peaks in the CVs of VK_3 and AQ-S. All the selected peaks are clear-cut and thus easily measured. The variation of permeability of quinones on the

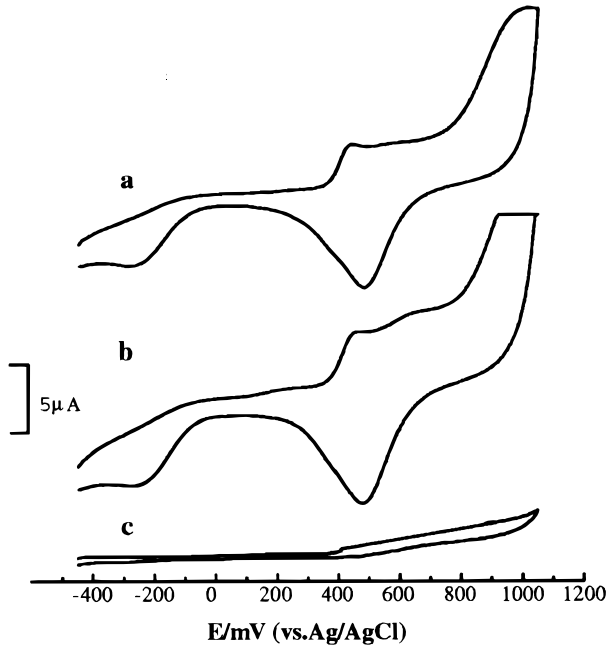

Figure 10. Cyclic voltammetric response of 5.0×10^{-4} mol/L AQ-S on bare gold (a), gold modified with pure MP SAM (b) and gold modified with mixed SAMs containing 80% MP (c). The supporting electrolyte was 0.1 mol/L $NaClO_4$ and 0.025mol/L phosphate buffer (pH 7.0). Scan rate was 50 mV/s.

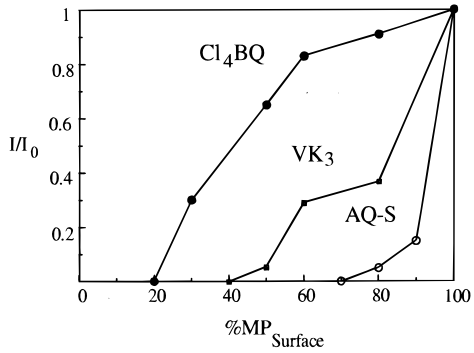

Figure 11. Permeability of three quinones on the mixed SAMs with different surface composition. The solid lines are provided as a guide to the eye.

SAMs with different composition is displayed in Figure 11. Clearly, when the surface component is same, the sequence of permeability of the three quinones on mixed SAMs is $Cl_4BQ > VK_3 >$ AQ-S.

4. Discussion

From the electrochemical measurements, we have demonstrated that mixed monolayers on gold containing $C_{12}SH$ and MP provide a convenient means of controlling electrochemical reaction of quinones at the SAMs-modified electrodes. The permeability of probe molecules could be tuned to some extent by varying the relative concentration of the two mercaptans in SAMs. We are making an effort to understand the origin of such variation of the permeability.

As yet, the surface composition of the two components in mixed SAMs is undetermined. The adsorption of long chain alkanethiolate at the gold surface is believed to be thermodynamically preferred because the van der Waals attraction among the polyethylene chain promotes formation of stable, two-dimensional crystalline structures at the surface of the substrate.[1−5] Some researchers suggest that the composition of monolayers adsorbed from solutions containing mixtures of alkanethiols should be determined principally by thermodynamics, although the mechanisms by which the components in the monolayer and in solution are equilibrated remains unclear. The corollary for the thermodynamic controlled structure is that the surface-adsorbed small molecule (MP here) should be substituted by the long chain alkanethiol ($C_{12}SH$ here) after infinite long time equilibrium. Anyhow, our results indicate that such equilibrium is not reached in the SAMs mixed with long chain and aromatic mercaptans prepared under our conditions. We find that the surface composition obtained from the RA-IR data is almost linearly related to the composition of the assembling solution, suggesting that the monolayers are far from thermodynamic equilibrium. The procedures for two components at the surface and in solution equilibrated at the interface require desorption of the small molecule from the substrate so that it might be substituted by the long chain molecule. However, the small molecule may not readily desorb from the substrate because they are anchored to the gold surface by the Au−S covalent bond. Actually, experiments[18,78] of exchange alkanethiol on gold surface by another kind of thiol from solution have demonstrated that quite a long time is needed to reach equilibrium (usually longer than 10 days). Since we prepared the mixed SAMs for only 12 h, we conclude that the surface composition in our SAMs is kinetically controlled.

Porter has suggested that electron transferring to solution species at the SAMs-modified electrodes could occur in three ways:[43] (1) the electron could transfer through the film via a tunneling process, (2) the electroactive species could permeate through the monolayer and react at the electrode surface, and (3) the electroactive species could diffuse to a bare spot (pinhole) on the electrode. It is known that the self-assembly of alkanethiols at the gold surface is very fast and gives almost perfect monolayers in very few hours. Thus, the third route could be ruled out in our case. SAMs from long chain alkanethiols have the advantage of forming highly ordered structure, on which the electron transfer is believed to adopt the first route. On the mixed SAMs prepared of long chain alkanethiols and aromatic thiols by coadsorption, we think the second route should be the main way that the electron-transfer reaction occurs. The aromatic mercaptan (MP here) acts as active sites for the electrochemical reaction. On this basis, the electrochemical response of probe molecules should depend on the distribution of the two components in the monolayer.

It is essential to discuss how the two components are distributed in the monolayers. We do not think the two components are uniformly distributed in the SAMs. As we have mentioned above, infrared spectroscopic investigation has revealed that ordered $C_{12}SH$ domain structure even exists while the mole fraction of MP in the film increases to 80%. Meanwhile, the electrochemical response of the three quinones on the SAMs also supports the existence of MP domain in the SAMs. A reasonable requirement for active sites to accomplish the electron transfer is that they should have similar size as the probe molecules. It is known that both VK_3 and AQ-S are larger than MP, so they cannot react at an active site containing only one or very few MP molecules. Undoubtedly, the electrochemical reaction of either VK_3 or AQ-S could occur only on a large MP domain. On this basis, the origin of different permeabilities of various quinones on the mixed SAMs should related to the size of the MP domain. Therefore, we also provide a convenient method to estimate the domain size of aromatic mercaptan in mixed SAMs. For example, the mixed SAM that has 80% MP

affects very slightly the reaction of Cl_4BQ, but partly inhibits that of VK_3 and almost fully inhibits that of AQ-S. It is reasonable to propose that the average size of active sites in the above SAMs is very possibly larger than the diameter of MP but smaller than that of AQ-S. If we consider the factor that some part of the MP domain should be covered by the neighboring $C_{12}SH$ molecules owing to the random orientation at the boundary of domains, the real size of MP domains should be even larger than the size of active sites felt by the probes. Consequently, we can propose that the average diameter of the MP domain should be around several nanometers. Although the domain structure mentioned above is not directly observed in this work, we note that our hypothesis is strongly supported by some recent SPM investigation on mixed SAMs.[79−81] In these reports, ordered nanometer scale domains have been directly observed with SPM.

5. Conclusions

Self-assembled monolayers of pure and binary mixtures of MP and $C_{12}SH$ with varied ratio are prepared on gold. Our research revealed that the composition of the mixed monolayers could be controlled by the ratio of MP and $C_{12}SH$ in the assembled solutions. The composition of monolayers prepared under our condition appears to be determined mostly by kinetics. Our result suggests that the mixed SAMs might contain nanometer scale MP domain. On such SAMs, the permeabilities of various quinones probes are different, which is predominated by the geometry of the quinones. The origin of the geometry-dependent permeability of probes is believed to be related to the average size of MP domain in SAMs.

The matrix formed by coadsorption of aromatic and long chain mecaptans on gold electrodes, which exhibits permselectivity to probe quinones, offers the prospect of using this approach to develop highly sensitive and selective electrochemical sensors for organic and biological samples. On the basis of the simplicity in the fabrication of such selective electrodes, its potentially applicable area in electrochemical analysis is believed to be wide.

Acknowledgment. Authors appreciate the financial support from the National Natural Science Foundation of China (NSFC). RA-IR spectra and contact angle were measured at the Center for Intelligent Material Research (CIMR) of Peking University. Valuable discussion from Dr. Gao Zuo-Ning is also greatly appreciated.

References and Notes

(1) Ulman, A. *An Introduction to Ultrathin Organic Films, From Langmuir-Boldgett to Self-Assembly*; Academic Press: San Diego, CA, 1991.
(2) Dubios, L. H.; Nuzzo, R. G. *Annu. Rev. Phys. Chem.* **1992**, *43*, 437.
(3) Bain, C. D.; Evans, S. D. *Chem. Br*. **1995**, 46.
(4) Zhong, C. J.; Porter, M. D. *Anal. Chem*. **1995**, 709A.
(5) Ulman, A. *Chem. Rev.* **1996**, *96*, 1533.
(6) Allara, D. L.; Parikh, A. N.; Judge, E. *J. Chem. Phys*. **1994**, *100*, 1761.
(7) Collazo, N.; Rice, S. A. *Langmuir* **1991**, *7*, 3144.
(8) Di Meglio, J. M.; Shanahan, M. E. R. C. R. *Acad. Sci. Paris II* **1993**, *316*, 1543.
(9) Bard, A. J.; Abruna, H. D.; Chidsey, C. E.; Faulkner, L. R.; Feldberg, S. W.; Itaya, K.; Majda, M.; Melroy, M.; Murray, R. W.; Porter, M. D.; Soriage, M. P.; White, H. S. *J. Phys. Chem*. **1993**, *97*, 7147 and references therein.
(10) Evans, S. D.; Sharma, R.; Ulman, A. *Langmuir* **1991**, *7*, 156.
(11) Labinis, P. E.; Fox, M. A.; Folkers, J. P.; Whitesides, G. M. *Langmuir* **1991**, *7*, 3167.
(12) Bain, C. D.; Whitesides, G. M. *Science* **1988**, *240*, 62.
(13) Overney, R. M.; Frommer, J.; Brodbeck, D.; Ruthi, R.; Howald, L.; Guntherrodt, H. J.; Fujihira, M.; Takano, H.; Gotoh, Y. *Nature* **1992**, *359*, 133.
(14) Biebuyck, H. A.; Whitesides, G. M. *Langmuir* **1993**, *9*, 1766.
(15) Troughton, E. B.; Bain, C. D.; Whitesides, G. M.; Nuzzo, R. G.; Allara, D. L.; Porter, D. L. *Langmuir* **1988**, *4*, 365.
(16) Laibinis, P. E.; Whitesides, G. M. *J. Am. Chem. Soc*. **1992**, *114*, 1990.
(17) Silberzan, P.; Leager, L.; Ausserre, D.; Benattar, J. *Langmuir* **1991**, *7*, 1647.
(18) Bain, C. D.; Evall, J.; Whitesides, G. M. *J. Am. Chem. Soc*. **1989**, *111*, 7155.
(19) Bain, C. D.; Whitesides, G. M. *J. Am. Chem. Soc*. **1989**, *111*, 7164.
(20) Chidsey, C. E. D.; Bertozzi, C. R.; Putvinski, T. M.; Mujsce, A. M. *J. Am. Chem. Soc*. **1990**, *112*, 4301.
(21) Chiedsey, C. E. D. *Science* **1991**, *251*, 919.
(22) Collard, D. M.; M. A. *Langmuir* **1991**, *7*, 1191.
(23) Rowe, G. K.; Creager, S. E. *Langmuir* **1991**, *7*, 2307.
(24) Bain, C. D.; Whitesides, G. M. *Langmuir* **1989**, *5*, 1370.
(25) Ulman, A.; Evans, S. D.; Shidman, Y.; Sharma, R.; Eilers, J. E.; Chang, J. C. *J. Am. Chem. Soc*. **1991**, *113*, 1499.
(26) Prime, K. L.; Whitesides, G. M. *Science* **1991**, *252*, 1164.
(27) Pale-Grosdemange, C.; Simon, E. S.; Prime, K. L.; Whitesides, G. M. *J. Am. Chem. Soc.* **1991**, *113*, 12.
(28) Haussling, L.; Michel, B.; Ringdorf, H.; Rohrer, H. *Angew. Chem., Int. Ed. Engl*. **1991**, *30*, 569.
(29) Sanassy, P.; Evans, S. D. *Langmuir* **1993**, *9*, 1024.
(30) Parikh, A. N.; Liedberg, B.; Atre, S. V.; Ho, M.; Allara, D. L. *J. Phys. Chem*. **1995**, *99*, 9996.
(31) Folkers, J. P.; Laibinis, P. E.; Whitesides, G. M. *Langmuir* **1992**, *8*, 1330.
(32) Folkers, J. P.; Laibinis, P. E.; Whitesides, G. M. *J. Adhes. Sci. Technol*. **1992**, *6*, 1397.
(33) Bumm, L. A.; Arnold, J. J.; Cygan, M. T.; Dunbar, T. D.; Burgin, T. P.; Jones, L.; Allara, D. L.; Tour, J. M.; Weiss, P. S. *Science* **1996**, *271*, 1705.
(34) Stranick, S. J.; Parikh, A. N.; Tao, Y. T.; Allara, D. L.; Weiss, P. S. *J. Phys. Chem*. **1994**, *98*, 7636.
(35) Allara, D. L. *Biosens. Bioelectron.* **1995**, *10*, 771.
(36) Laibinis, P. E.; Nuzzo, R. G.; Whitesides, G. M. *J. Phys. Chem*. **1992**, *96*, 5097.
(37) Rowe, G. K.; Creager, S. E. *Langmuir* **1994**, *10*, 1186.
(38) Rubinstein, I.; Steinberg, S.; Tor, Y.; Shanzer, A.; Sagiv, J. *Nature* **1988**, *332*, 426.
(39) Bilewicz, R.; Majda, M. *J. Am. Chem. Soc*. **1991**, *113*, 5464.
(40) Chailapakul, O.; Crooks, R. M. *Langmuir* **1993**, *9*, 884.
(41) Becka, A. M.; Miller, C. J. *J. Phys. Chem*. **1992**, *96*, 2657.
(42) Cheng, Q.; Brajter-Toth, A. *Anal. Chem*. **1992**, *64*, 1998.
(43) Porter, M. D.; Bright, T. B.; Allara, D. L.; Chidsey, C. D. E. *J. Am. Chem. Soc*. **1987**, *109*, 3559.
(44) Bard, A. J.; Faulkner, L. R. *Electrochemical Methods, Fundamentals and Applications*; John Wiley & Sons: New York, 1980.
(45) Bard, A. J. *Electroanalytical Chemistry*; Marcel Dekker: New York, 1976; Vol. 9, p 125.
(46) Lord, R. C.; Marston, A. L.; Miller, F. A. *Spectrochim. Acta* **1957**, *9*, 113.
(47) Miller, G.; Guiliano, M.; Kister, J.; Chouteau, J.; Metzger, J. *Spectrochim. Acta* **1980**, *36A*, 713.
(48) Sathyanarayana, D. S.; Raja, S. V. K. *Spectrochim. Acta* **1985**, *41A*, 809.
(49) Nowak, M. J.; Rostkowska, H.; Lapinski, L.; Leszczynski, J.; Kwiatkowski, J. S. *Spectrochim. Acta* **1991**, *47A*, 339.
(50) Shunmuqam, R.; Sathyanarayana, D. N. *Bull. Soc. Chim. Belg.* **1984**, *93*, 121.
(51) Stoyanov, S.; Petkov, I.; Antnov, L.; Stoyanova, T.; Karagiannidis, P.; Aslanidis, P. *Can. J. Chem*. **1990**, *68*, 1482.
(52) Shumugam, R.; Sathyanarayana, D. N. *Spectrochim. Acta* **1984**, *40A*, 757.
(53) Penfold, B. R. *Acta Crystallogr*. **1953**, *6*, 707.
(54) Snyder, R. G.; Strauss, H. L.; Elliger, C. A. *J. Phys. Chems*. **1982**, *86*, 5145.
(55) Snyder, R. G.; Maroncelli, M.; Strauss, H. L. *J. Phys. Chems*. **1986**, *90*, 5623.
(56) Nuzzo, R. G.; Korenic, E. M.; Dubois, L. H. *J. Chem. Phys*. **1990**, *93* (1), 767.
(57) Stole, S. M.; Porter, M. D. *Langmuir* **1990**, *6*, 1199.
(58) Adamson, A. W.; Ling, I. *Adv. Chem. Ser*. **1964**, *43*, 57.
(59) Young, T. *Miscellaneous Works*; Peakock, G., Ed.; Murry: London, 1855; Vol. 1, p 418.
(60) Cassie, A. B. D.; Baxter, S. *Trans. Faraday Soc.* **1944**, *40*, 546.
(61) Cassie, A. B. D. *Discuss. Faraday Soc.* **1948**, *3*, 11.
(62) Bain, C. D.; Whitesides, G. M. *J. Am. Chem. Soc*. **1988**, *110*, 5897.

(63) Silbernan, P.; Leger, L.; Ausserre, D.; Benattar, J. J. *Langmuir* **1991**, *7*, 1647.
(64) Wasserman, S. R.; Tao, Y. T.; Whitesides, G. M. *Langmuir* **1989**, *5*, 1074.
(65) Le Grange, J. D.; Markham, J. L.; Kurkjian, C. R. *Langmuir* **1993**, *9*, 1749.
(66) Maoz, R.; Sagiv, J. *J. Colloid Interface Sci*. **1984**, *100*, 465.
(67) Carson, G.; Granick, S. *J. Appl. Polym. Sci*. **1989**, *37*, 2767.
(68) Kessel, C. R.; Granick, S. *Langmuir* **1991**, *7*, 532.
(69) Ulman, A. *Adv. Mater*. **1990**, *2*, 573.
(70) Sondag-Huethorst, J. A. M.; Fokkink, L. G. J. *Langmuir* **1992**, *8*, 2560.
(71) Sondag-Huethorst, J. A. M.; Fokkink, L. G. J. *J. Electroanal. Chem*. **1994**, *367*, 49.
(72) Miller, C.; Cuendet, P.; Gratzel, M. *J. Phys. Chem*. **1991**, *95*, 877.
(73) Becka, A. M.; Miller, C. J. *J. Phys. Chem*. **1993**, *97*, 6233.
(74) Oesch, U.; Janata, J. *Electrochim. Acta* **1983**, *28*, 1237.
(75) Bailey, S. L.; Ritchie, I. M. *Electrochim Acta* **1985**, *30*, 3.
(76) Takehara, K.; Takemure, H.; Ide, Y. *J. Colloid Interface Sci*. **1993**, *156*, 274.
(77) Li, J. H.; Liu, Z. M.; Dong, S. J.; Wang, E. K. *Chem. Res. Chin. Univ*. **1996**, *12*, 340.
(78) Collard, D. M.; Fox, M. A. *Langmuir* **1991**, *7*, 1192.
(79) Sato, Y.; Yamada, R.; Mizutani, F.; Uosaki, K. *Chem. Lett*. **1997**, *13*, 987.
(80) Tamada, K.; Hara, M.; Sasabe, H.; Knoll, W. *Langmuir* **1997**, *13*, 1558.
(81) Imabayashi, S. I.; Hoara, D.; Kakiuchi, T. *Langmuir* **1997**, *13*, 4502.